Structure–activity relationships of the antimicrobial peptide gramicidin S and its analogs: Aqueous solubility, self-association, conformation, antimicrobial activity and interaction with model lipid membranes

Thomas Abraham [a], Elmar J. Prenner [a,1], Ruthven N.A.H. Lewis [a], Colin T. Mant [b], Sandro Keller [c], Robert S. Hodges [b], Ronald N. McElhaney [a,*]

[a] Department of Biochemistry, University of Alberta, Edmonton, Alberta T6G 2H7, Canada
[b] Department of Biochemistry and Molecular Genetics, University of Colorado at Denver and Health Sciences Center, Aurora, CO 80045, USA
[c] Molecular Biophysics, University of Kaiserslautern, Erwin-Schrodinger-Str. 13, 67663 Kaiserslautern, Germany

ARTICLE INFO

ABSTRACT

GS10 [cyclo-(VKL*d*YPVKL*d*YP)] is a synthetic analog of the naturally occurring antimicrobial peptide gramicidin (GS) in which the two positively charged ornithine (Orn) residues are replaced by two positively charged lysine (Lys) residues and the two less polar aromatic phenylalanine (Phe) residues are replaced by the more polar tyrosine (Tyr) residues. In this study, we examine the effects of these seemingly conservative modifications to the parent GS molecule on the physical properties of the peptide, and on its interactions with lipid bilayer model and biological membranes, by a variety of biophysical techniques. We show that although GS10 retains the largely β-sheet conformation characteristic of GS, it is less structured in both water and membrane-mimetic solvents. GS10 is also more water soluble and less hydrophobic than GS, as predicted, and also exhibits a reduced tendency for self-association in aqueous solution. Surprisingly, GS10 associates more strongly with zwitterionic and anionic phospholipid bilayer model membranes than does GS, despite its greater water solubility, and the presence of anionic phospholipids and cholesterol (Chol) modestly reduces the association of both GS10 and GS to these model membranes. The strong partitioning of both peptides into lipid bilayers is driven by a large favorable entropy change opposed by a much smaller unfavorable enthalpy change. However, GS10 is also less potent than GS at inducing inverted cubic phases in phospholipid bilayer model membranes and at inhibiting the growth of the cell wall-less bacterium *Acholeplasma laidlawii* B. These results are discussed in terms of the comparative antibiotic and hemolytic activities of these peptides.

© 2013 Elsevier B.V. All rights reserved.

1. Introduction

The structure, physical properties and mechanism of action of antimicrobial peptides have been the focus of considerable fundamental and applied research interest in recent years [1–3]. Antimicrobial peptides are produced by a number of microorganisms and are widely distributed in animals and plants, where they form part of the innate immune defense mechanism of the host species. Antimicrobial peptides are currently being investigated as potential sources of novel therapeutic antibiotics to combat the increasing numbers of microorganisms resistant to conventional antibiotics [1–5]. They exist in a wide variety of structural motifs (α-helical, β-sheet, linear and cyclic), [6,7] but almost all are cationic amphiphilic molecules which can interact with the bacterial inner membrane, the lipid bilayer of which appears to be their primary target. The mode of action of most antimicrobial peptides is thought to involve initial electrostatic interaction between anionic phospholipids on the outer monolayer of the bacterial membrane and the cationic amino acid residues of the peptide, followed by partial penetration of the peptide into the lipid bilayer, thus allowing the hydrophobic amino acid residues of the peptide to contact the hydrocarbon chains of the phospholipids. These peptides are believed to kill bacteria by compromising the structural and functional integrity of the phospholipid bilayer of the target membrane [1–7].

The antimicrobial peptide gramicidin S (GS) was first isolated from the Gram-positive bacterium *Bacillus brevis* [8] and is one of a series of antimicrobial peptides produced by that organism [9,10]. GS is a cyclic cationic decamer (primary structure *cyclo*[VOL*d*FPVOL*d*FP]) in which

the two tripeptide sequences Val-Orn-Leu form antiparallel β-sheets terminated on each side by a type II β-turn formed by the two D-Phe-Pro sequences. It thus folds into a fairly rigid amphipathic structure in which the two polar positively charged Orn side chains project from one side and the four hydrophobic Leu and Val side chains project from the other side (Fig. 1). This structure is stabilized by cross-ring intramolecular hydrogen bonds, involving the amide protons and carbonyl groups of the two Leu and two Val residues [9,10]. GS is a powerful antibiotic against a broad range of Gram-negative and Gram-positive bacteria as well as against several pathogenic fungi [9,10]. However, GS is also highly hemolytic and as a result, its therapeutic use is restricted to topical applications [8]. Structure–activity studies of GS analogs have shown that the expression of antibiotic activity is contingent upon the retention of a β-sheet conformation in which cationic and hydrophobic side chains are segregated on opposite faces of the molecule [9,10].

A great deal of evidence exists that the major target of GS is the lipid bilayer of bacterial or erythrocyte membranes and that this peptide kills bacteria cells and lyses erythrocytes by permeabilizing and destabilizing their cytoplasmic membranes [1,9–11]. We have studied the interaction of GS with a variety of lipid bilayer model membranes using a number of biophysical techniques in order to determine the molecular mechanism of action [10,11]. In particular, DSC studies have shown that GS more strongly perturbs the thermotropic phase behavior of anionic as compared to zwitterionic phospholipid bilayers and of more fluid as compared to less fluid membranes [12], and densitometry and sound velocity studies indicate that GS incorporation decreases the density and volume compressibility of the host phospholipid bilayer by increasing the conformational disorder and motional freedom of the phospholipid hydrocarbon chains [13]. ^{31}P NMR [14] and X-ray diffraction [15] studies also indicate that GS at low concentrations causes the thinning of phospholipid bilayers and can induce the formation of inverted nonlamellar cubic phases in phospholipid dispersions at higher concentrations. FTIR spectroscopic studies also show that GS is located in the polar/apolar interfacial region of phospholipid bilayers and that it penetrates more deeply into anionic and more fluid bilayers [16]. As well, several physical techniques indicate that the presence of Chol attenuates all of the above effects of GS on phospholipid bilayers, at least in part by reducing the penetration of this peptide into these model membranes [16,17]. Finally, a solid-state ^{19}F NMR study of a ^{19}F-labeled GS analog suggests that the GS molecule is aligned with its cyclic β-sheet lying flat in the plane of the bilayer, with its polar and positively charged Orn residues projecting toward the bilayer surface, where they can interact with negatively charged phosphate headgroups of the phospholipid molecules, while the four hydrophobic Val and Leu residues project toward the bilayer center, where they interact with the phospholipid hydrocarbon chains [18]. The location and orientation of GS as deduced from the biophysical studies noted above are both consistent with the results of recent electrophysiological experiments demonstrating that GS increases the conductivity of phospholipid black lipid membranes without the formation of discrete pores or channels [19].

We have also shown that strongly antimicrobial GS analogs with markedly reduced hemolytic activity can be obtained by simultaneously altering both the ring size and the enantiomeric conformation of key amino acid residues [20–23], thus opening the way for the possible development of further GS analogs for use as potent oral or injectable broad-spectrum antibiotics [24]. The parent compound for these diastereomeric ring-size analogs is GS10, in which the two relatively polar and positively charged Orn residues of GS were replaced by the slightly less polar but still positively charged Lys residues, and the two less polar aromatic Phe residues were replaced by the more polar aromatic Tyr residues (Fig. 1). These conservative changes in the GS molecule were implemented in order to increase the aqueous solubility of GS10 analogs and to introduce an intrinsic fluorescent label so that non-perturbing spectroscopic experiments can be performed (Tyr for Phe substitutions), and to make them less expensive to synthesize (Lys for Orn substitutions), hopefully without significantly altering the conformation, physical properties and antibiotic activity. In fact, GS10 does seem to retain the β-sheet conformation of GS and to exhibit at least roughly comparable antibiotic and hemolytic activities [20–24]. However, the conformations and relative amphipathicities of GS and GS10 have not been previously determined under strictly comparable conditions, and the effect of GS10 on the lamellar/nonlamellar phase propensity of phospholipid model membranes and its antibiotic activity against the cell wall-less Mollicute *Acholeplasma laidlawii* B relative to GS itself, have also not been studied. These comparisons are important for a full understanding of the relationship of the structure and physical properties of these two antimicrobial peptides to their antimicrobial activities, since GS10 rather than GS serves as the platform for the development of promising diastereomeric ring-size analogs. In this regard, it is important to separate changes resulting from alterations in the amino acid composition of GS10 relative to GS itself from changes resulting from ring expansion and enantiomeric inversions in the various GS10 analogs. As well, we also present ITC results for the binding of GS and GS10 to a variety of phospholipid model membranes and compare the results obtained to previous ITC studies of GS itself [25] and of GS14dK_4, a diastereomeric ring-size analog exhibiting a highly retained antimicrobial activity but a markedly reduced hemolytic potency [26].

2. Materials and methods

2.1. Lipid and peptides

Phospholipids and Chol were purchased from Avanti Polar Lipids Inc. (Alabaster, AL, USA) and used without further purification. Linear derivatives of the required cyclic peptides were synthesized by solid-phase methods using t-butyloxycarbonyl chemistry and then N- to C- (Pro at the C-terminus) terminally cyclized in solution, as described previously [27]. The products were then purified and analyzed by RP-HPLC and their final purity determined by mass spectrometry. Stock solutions of the pure peptides were prepared in methanolic solution and their concentrations determined by amino acid analysis ($\pm 5\%$ error). Aqueous solutions of these peptides were then prepared by drying down known volumes of the stock solution and subsequently redissolving the peptide film in an appropriate volume of aqueous buffer to obtain the peptide concentration required. Unless otherwise stated, all experiments were performed in a buffer composed of 50 mM Tris, 150 mM NaCl and 1 mM NaN$_3$, pH 7.4.

2.2. Circular dichroism

CD spectra were recorded with a Jasco J-720 spectropolarimeter (Easton, MD) using quartz cells of 2 mm path length. The spectra were measured using ~50 μM peptide solutions in aqueous- (10 mM

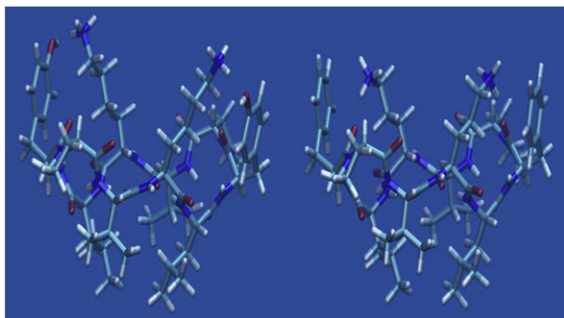**Fig. 1.** The chemical structures and conformations of GS10 (left) and GS (right) shown edge-on to the plane of the cyclic decapeptide ring. The two positively charged Lys (GS10) or Orn (GS) amino acid residues are shown projecting upwards and the four hydrophobic Leu and Val residues are shown projecting downward. Carbon atoms are shown in green, hydrogen atoms in white, oxygen atoms in red and nitrogen atoms in blue.

acetate, pH 5.5), and in TFE-containing (10 mM acetate, pH 5.5 in 50 vol.% TFE) buffer at 20 °C.

2.3. RP-HPLC

Reversed-phase high performance liquid chromatographic analyses were performed on a Zorbax 300SB-C8 column (150 × 2.1-mm inner diameter, 3.5 μm particle size, 300 Å pore size; Rockland Technologies, Wilmington, DE) using an Agilent 1100 liquid chromatograph (Agilent Technologies, Little Falls, DE) with a linear AB gradient of 0.5% B/min (solvent A: 0.2% aqueous trifluoroacetic acid; solvent B: 0.18% trifluoroacetic acid in acetonitrile) at a flow rate of 0.3 ml/min. Retention times were recorded at temperatures between 5 °C and 80 °C (3 °C increments) using the temperature profiling RP-HPLC protocols described previously [28].

2.4. ^{31}P NMR spectroscopy

^{31}P-NMR spectra were recorded as a function of temperature with a Varian Unity-300 spectrometer operating at 121.41 MHz for ^{31}P, using data acquisition and data processing protocols similar to those described previously [14]. Peptide-free and peptide-containing DPEPE vesicles (with and without Chol) were also prepared for ^{31}P NMR spectroscopy using the same methods previously used in this laboratory [14].

2.5. Antimicrobial activity

The cell wall-less Mollicute *A. laidlawii* B was cultured in chloroform-extracted BSA-free media and cell growth was monitored turbidometrically [29]. The effect of the antimicrobial peptides on cell growth was monitored as a function of time after the addition of these peptides to the culture medium just prior to a 10% (by volume) inoculation with cells in the mid log phase of growth. Cell growth was expressed as a percentage of the maximum growth obtained in the absence of a peptide. Growth yields were plotted as a function of peptide concentration and growth inhibitory activity was expressed in terms of an apparent LD_{50} using methods similar to those previously utilized in this laboratory [30].

2.6. High-sensitivity isothermal titration calorimetry

The heat flow resulting from the association of the peptide to lipid vesicles was measured using a high-sensitivity VP-ITC instrument (Microcal LLC, Northampton, MA) with a reaction cell volume of 1.448 ml [31]. Prior to use, solutions were degassed under vacuum (140 mbar, 8 min) to eliminate air bubbles. The data were acquired by computer software developed by MicroCal LLC. Titration calorimetric experiments were performed as follows. The peptide solution (25–60) was placed in the calorimeter cell and the lipid vesicles (2.5–38 mM) were injected via the titration syringe in aliquots of 4–10 ml. Each injection produced a heat of reaction, which was determined by integration of the heat flow tracings. This mode is capable of providing both the binding isotherm and the total binding enthalpy [31–33].

The heat of dilution was determined in control experiments by injecting the corresponding vesicle dispersion into the buffer solution. The heats of dilution were subtracted from the heats determined in the corresponding peptide–lipid titration experiments. The overall association enthalpy and association isotherm were determined from these peptide–lipid titration experiments using standard procedures [31–33] and the data were analyzed and fitted as described [34]. Since our dynamic light scattering experiments and the results of other studies indicated that these antimicrobial peptides do not cause the fusion or disruption of the LUVs utilized in the ITC titrations under the experimental conditions employed here, we used half of the total lipid concentration in the estimation of the degree of association and the

determination of the thermodynamic association parameters, since these antimicrobial peptides appear to initially have access only to the outer monolayer of the phospholipid bilayer.

The single- and multi-component large unilamellar lipid vesicles used in these ITC studies were prepared as follows. In a typical experiment, specified amounts of lipid (~60 mg) were first dried under reduced pressure (vacuum) overnight. The lipid was then hydrated with an appropriate amount of buffer (~2 ml) and the dispersion thus formed was subjected to vortex mixing at temperatures well above the gel/liquid-crystalline phase transition temperature of the phospholipids. The multilamellar vesicles thus obtained were then freeze–thawed several times. These vesicles were then extruded through a small volume extrusion apparatus (Avestin Inc., Ottawa, Canada) equipped with polycarbonate membrane filter (19 mm diameter, 200 nm pore diameter) about 25 times, in order to produce LUVs of vesicle size ~200 nm. Lipid concentrations were determined by gas chromatography using an appropriate internal standard (±5% error). The same procedure was followed for two-component vesicles, except that appropriate quantities of each component (lipid or Chol) were first co-dissolved in chloroform and thoroughly mixed prior to vesicle preparation.

2.7. Dynamic light scattering

The average hydrodynamic diameter of pure and peptide-bound LUVs were measured by a Brookhaven BI-90 particle Analyzer (Brookhaven Instruments, Holtsville, NY) equipped with disposable square cells. The solutions were subjected to scattering by a monochromatic light (10 mW He–Ne laser, wavelength = 632.4 nm) and the scattered light intensity was measured at a scattering angle of 90°.

3. Results

3.1. Reversed-phase HPLC studies

The binding affinity of a peptide to a RP-HPLC column is determined by its effective hydrophobicity, with more hydrophobic peptides exhibiting stronger binding to the hydrophobic stationary phase and thus greater retention times [28]. Illustrated in Fig. 2A are plots of the absolute RP-HPLC retention times of GS10 as a function temperature. For comparative purposes, similar plots for GS are also presented. The RP-HPLC retention times of GS10 are significantly shorter than those of GS, indicating that GS10 has a lower propensity for binding to hydrophobic surfaces under all conditions examined. Given the structural and conformational similarities between GS and GS10, these differences in retention times undoubtedly reflect differences between the intrinsic hydrophobicities of these two molecules due to their different amino acid compositions. Specifically, the replacement of the two Phe residues of GS by the more polar Tyr residues would be expected to decrease the hydrophobicity of GS10 relative to GS itself, despite the fact that the two Orn residues of GS are replaced by slightly more hydrophobic Lys residues in GS10.

Fig. 2A also shows that the retention times of both GS and GS10 on RP-HPLC columns exhibit a biphasic response to temperature change. At low temperatures (<45–50 °C), the retention times of GS and GS10 increase with temperature up to a maximal value near 45–50 °C, beyond which further increases in temperature are accompanied by monotonic decreases in RP-HPLC retention times. In cases where increases in temperature are not accompanied by the exposure of occluded hydrophobic surfaces, peptide RP-HPLC retention times actually decrease monotonically with temperature (for an example, see the plot for the linear reference peptide shown Fig. 2A and B), because of the effects arising from thermally induced decreases in solvent viscosity, increases in solute diffusivity and mass transfer, etc. [28]. However, whenever increases in temperature also increase the probability of exposing occluded hydrophobic surfaces, the thermally induced decrease
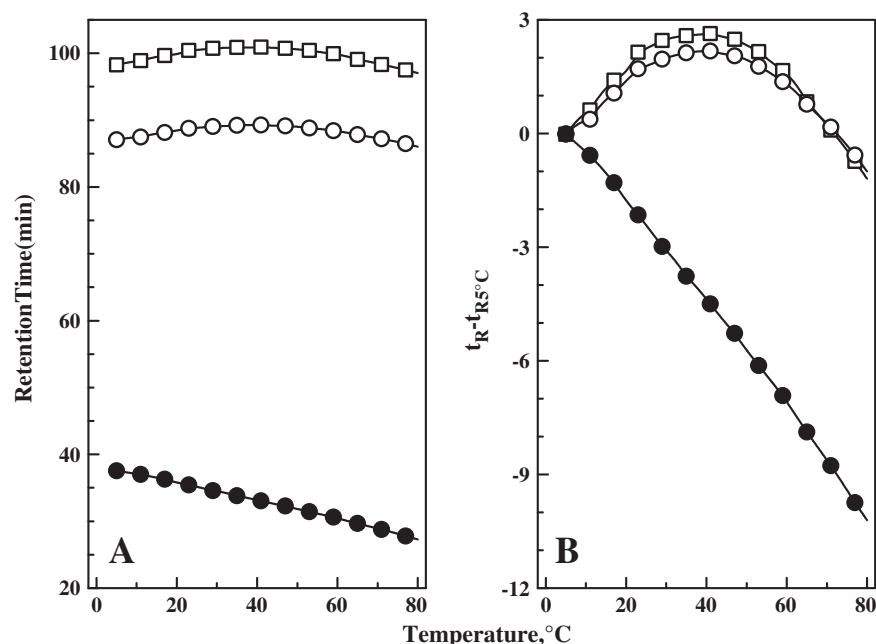
Fig. 2. Temperature-profiling HPLC studies of the peptides GS and GS10. Comparable data are also presented for the linear non-associating peptide, AKAKA*d*YPAKAKA*d*YP which serves as a reference for these studies. Plots of absolute RP-HPLC retention times are presented in panel A and plots of RP-HPLC retention times relative to values measured at 5 °C are presented in Panel B. Data are presented for the peptides, Gramicidin S (□), GS10 ((○) and the non-associating reference (●).

in RP-HPLC retention times will be attenuated and retention times may even increase with temperature, depending on the nature of the process involved and the relative sizes of the thermally exposed hydrophobic surfaces [28]. For conformationally stable peptides such as GS and GS10, a change in the degree of self-association is the only process whereby a thermally induced exposure of occluded hydrophobic surfaces can occur. Consequently, we can interpret a positive deviation of the temperature dependence of the RP-HPLC retention times of these peptides relative to that of a non-associating reference in terms of changes in the propensity of the peptide to self-associate in aqueous media. This novel "RP-HPLC temperature profiling" approach to assessing peptide self-association has been successfully applied to amphipathic cyclic β-sheet peptides based on gramicidin S [24,28], amphipathic α-helical peptides, including monitoring of unfolding of the α-helix to random coil with increasing temperature [35], and amphipathic α-helical peptides that form two-stranded α-helical coiled-coils [36]. Significantly, the profiling results with the latter peptides also correlated with coiled-coil stability determined by well-established biophysical approaches. This now established method has also helped further the development of antimicrobial peptides due to its correlation with antimicrobial and hemolytic activities [37–40]. We can thus conclude from the results presented in Fig. 2A and B that GS and GS10 both exhibit appreciable propensities for self-association in aqueous buffer. Moreover, when the RP-HPLC retention times of GS and GS10 are plotted relative to those observed at 5 °C, it becomes apparent that at all temperatures below 60 °C, GS consistently exhibits larger deviations from the behavior of the non-associating reference than GS10 (Fig. 2B). This observation indicates that GS has a consistently higher propensity for self-association in aqueous buffer than GS10, although as gaged by the parameters plotted in Fig. 2B, the differences in the magnitudes of the self-association parameters of GS to GS10 are not drastic. These small differences between the self-association parameters of GS and GS10 probably reflect the relatively small changes in hydrophobicity incurred in replacing the Phe residues of GS with Tyr, and the fact that the location of the Phe residues at the edges of the hydrophobic face of GS is such that their replacement with Tyr would not markedly reduce the size of the contiguous hydrophobic surface of the peptide [41]. However, one should note that although the magnitude of differences

between the self-association parameters of GS and GS10 is small, the units of these parameters are actually HPLC retention times, which have an exponential relationship to the underlying thermodynamic equilibria and are thus reflecting disproportionally larger differences in association/dissociation equilibria of these peptides.

3.2. Circular dichroism studies

Illustrated in Fig. 3 is a comparison of the CD spectra exhibited by GS and GS10 in both aqueous and so-called membrane-mimetic media. 10 mM acetate buffer (pH 5.5) was used for these studies because, unlike GS10, GS was not sufficiently soluble in 10 mM phosphate buffer (pH 7.0) to enable the acquisition of the CD spectra of GS and GS10
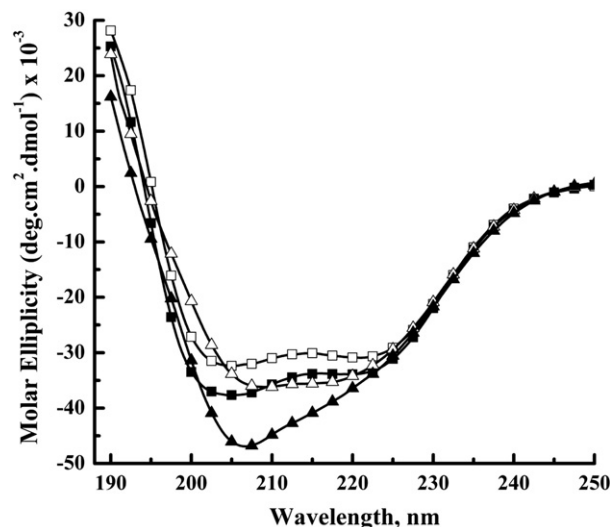

Fig. 3. CD spectra exhibited by GS and GS10 in aqueous and TFE-containing buffer. The spectra shown were acquired at peptide concentrations near 50 mM and are representative of: □ GS10 in aqueous buffer; △ GS10 in TFE-containing buffer; ■ GS in aqueous buffer; ▲ GS in TFE-containing buffer.

under comparable conditions. Fig. 2 shows that the contours of the molar ellipticity profiles exhibited by aqueous solutions of the two peptides are very similar, suggesting that they share many common conformational features. However, as noted previously [20,21], the molar ellipticity profiles of these peptides are atypical of proteins with a high β-sheet structure content, probably because of significant contributions from the relatively high content of β-turn structure (~40 residue %) and the aromatic residues (~20 residue %). However, the magnitudes of the molar ellipticities of GS and GS10 near 222 nm are quite large (~ −30,000), these values increase significantly when the peptides are transferred from aqueous to so-called membrane-mimetic media, and the molar ellipticity values of GS near 222 nm are always greater in magnitude than that of GS10 under comparable conditions. Also, GS exhibits a significantly greater change in its molar ellipticity profile upon transfer from aqueous to membrane-mimetic media than does GS10. We therefore conclude that these two peptides both retain a high degree of antiparallel β-sheet structure when dissolved in aqueous media, and that their secondary structure content increases when transferred to membrane-mimetic solvents (i.e., their secondary structures exhibit significant solvent inductibility). Nevertheless, GS10 is less structured than GS in both aqueous and membrane-mimetic media and less sensitive to changes in the polarity of the solvent than is GS. The probable physical basis and implications of these observations will be explored later in the Discussion.

3.3. A. laidlawii B growth inhibition studies

We study the effects of GS10 on the growth of the mycoplasma *A. laidlawii* B here because the absence of a cell wall in this bacterium makes the interpretation of the results obtained, and their comparison with the effects of GS10 on the various lipid bilayer model membranes studied here and previously, more straightforward. This is because some GS analogs exhibit weak antibiotic activity due to their strong binding to the cell walls of conventional bacteria, although they also bind strongly to and potently disrupt lipid bilayer model membranes [20,21,30]. The weak growth inhibiting abilities of these GS analogs are thus presumably due to the fact that high concentrations of these peptides must be added to saturate cell wall binding before an interaction with the lipid bilayer of the bacterial inner membrane can take place. Therefore, by studying the effects of GS10 on the growth of this organism, we can more accurately determine the "intrinsic" antimicrobial activity of GS and its various analogs.

The effects of GS10 on *A. laidlawii* B growth are briefly summarized below, along with comparable data obtained with GS itself and the weakly hemolytic GS ring-size analog GS14dK$_4$. The antibiotic activity of GS10 against *A. laidlawii* B (LD$_{50}$ ~0.65 mM) is significantly lower than that of GS (LD$_{50}$ ~0.17 mM), but somewhat higher than that of the weakly hemolytic GS14dK$_4$ (LD$_{50}$ ~1.2 mM), observations consistent with the results of previously published assays of the antimicrobial activities of these peptides against various Gram-negative and Gram-positive bacteria [20,21,30]. The relationship between the biological activity of GS10 and its capacity to interact with and perturb lipid membranes was examined in the spectroscopic and calorimetric measurements described below.

3.4. ^{31}P NMR spectroscopic studies

We have presented evidence in previous studies that GS and its ring-size analogs may destabilize lipid bilayer model and biological membranes in part by increasing negative monolayer curvature stress, thus promoting the formation of inverted cubic phases [14,15]. We have thus also studied the ability of GS10 to induce such phases in DPEPE aqueous dispersions. DPEPE is a particularly suitable phospholipid for investigating these effects, since it exhibits lamellar gel/liquid-crystalline and lamellar liquid-crystalline/inverted hexagonal phase transitions at 22 and 92 °C, respectively, thus providing a broad

temperature interval over which the peptide-induced formation of inverted lipid phases may be detected. Illustrated in Fig. 4A are representative ^{31}P NMR spectra exhibited by GS10- and GS-containing DPEPE vesicles as a function of temperature. At all temperatures from 25 to 85 °C, aqueous dispersions of DPEPE alone exhibit ^{31}P NMR spectra typical of unoriented liquid-crystalline phospholipid bilayers, in which lipid phosphate headgroups are undergoing fast axially symmetric motion, as expected in this temperature interval. At low temperatures, the spectra exhibited by peptide-free and peptide-containing (4 mol%) DPEPE membranes also exhibit spectra consistent with the presence of DPEPE bilayers. However, at high temperatures, all of the GS- and GS10-containing mixtures examined exhibit ^{31}P NMR spectra which contain a sharp peak centered near 2 ppm downfield (the isotropic component), which arises from the formation of an inverted cubic phase [14,15]. However, the temperature range over which this process occurs, and the extent to which it takes place, differ significantly between the two peptides. As illustrated in Fig. 4B, the growth of the isotropic component in Chol-free GS-containing DPEPE vesicles (T$_{50}$ ~52 °C) occurs over a lower temperature range and goes further toward completion than that of the corresponding GS10-containing sample (T$_{50}$ ~67 °C), indicating that GS has a greater propensity for inducing cubic phase formation. Fig. 3B also shows that in the presence of membrane Chol (30 mol%), GS- and GS10-induced cubic phase formation is shifted to higher temperatures (T$_{50}$ ~61 °C for GS vs T$_{50}$ ~80 °C for GS10), indicating that membrane Chol inhibits the capacity of these peptides to induce cubic phase formation in these membranes. However, the inhibitory effect of Chol is quantitatively greater in the GS10-containing system, indicating that Chol reduces the interactions of GS10 with DPEPE bilayers to a greater extent than that of GS itself. The probable thermodynamic basis of these and other differences between the properties of GS and GS10 are examined in the ITC studies presented below.

3.5. ITC studies

ITC is a quick, reliable and versatile thermodynamic technique for studying the association of antimicrobial peptides, detergents and other amphiphiles with lipid bilayer model membranes [42,43]. We have applied this technique here to investigate the interactions of GS and GS10 with a number of LUVs having different lipid compositions. In particular, we have studied the association of these two antimicrobial peptides with lipid vesicles composed of the zwitterionic phospholipid POPC, the anionic lipid POPG, and POPC/POPG mixtures (mole ratio 3:1), as well as mixtures of POPC/Chol and POPG/Chol (mole ratio 3:2). The ITC isotherms obtained in each case were then analyzed using a simple surface partition model. In this model, the Gouy–Chapman theory is utilized to calculate the peptide surface concentrations based on electrostatic interactions between the positively charged peptide molecules and initially neutral or anionic phospholipid polar headgroups, and then a surface/bilayer mole ratio partition coefficient (K_0) is determined [34]. K_0 thus represents the intrinsic or chemical component of the association process and is a measure of membrane affinity after correction for electrostatic effects. We present below the results of such an analysis for the association of GS and GS10 with POPC, POPC/POPG and POPC/Chol LUVs, where high-quality ITC data and good fits with the above model were possible. In the cases of POPG and POPG/Chol vesicles, both raw ITC data and model fits were much poorer, so we only make qualitative references to these results. The poorer quality of the data and the corresponding fits for these latter two vesicle systems likely result from effects such as an incomplete ionization of the phosphate moieties of the polar headgroups, to increased counterion binding, etc., due to their high negative surface charge density.

Representative ITC titrations of POPC LUVs into solutions of GS and GS10 are presented in Fig. 5A and C, respectively, and the plots of the normalized and integrated heats of association of these peptides with POPC (solid symbols) and POPC/Chol (open symbols) LUVs, and their
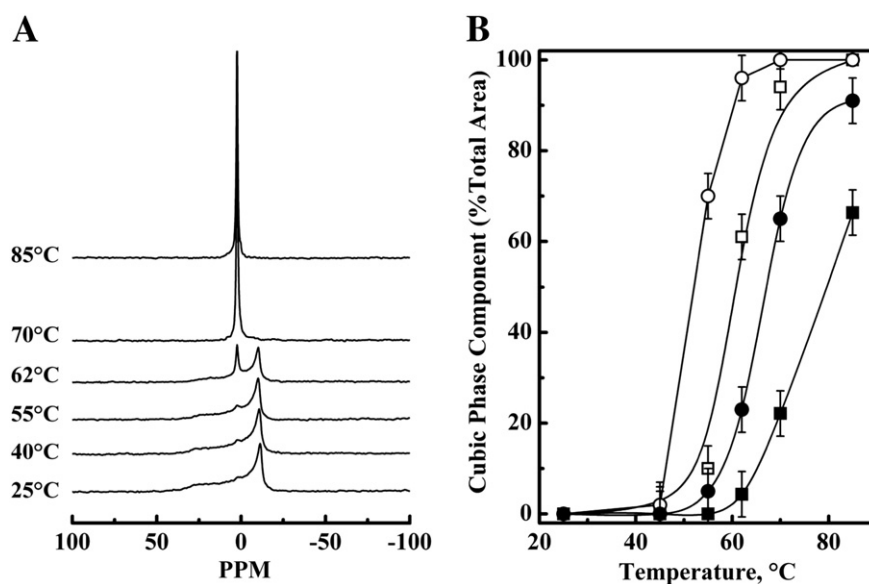
Fig. 4. ^{31}P NMR spectroscopic studies of the effect of GS and GS10 on the lamellar/nonlamellar phase behavior of DPEPE. Panel A is a representative data set illustrating temperature dependent changes in the ^{31}P NMR powder patterns exhibited by a DPEPE:GS mixture (25:1 mol:mol). Panel B shows the temperature dependent changes in the fractional area of the isotropic component observed in spectra exhibited by the following mixtures: ○ GS:DPEPE; ● GS:(DPEPE + Chol); □ GS10:DPEPE; ■ GS10:(DPEPE + Chol). All lipid:peptide ratios were 25:1 and the Chol-containing mixtures contained 30 mol% Chol.

fits to the model, are presented in Fig. 5B and D. The ITC titrations reveal that the initial endothermic heat of association decreases and levels off to a constant heat of dilution value as the peptide in solution becomes progressively associated with the lipid vesicles added to the sample cell, and the good fit of the model to the experimental heats of peptide/vesicle association are illustrated by the closeness of the solid
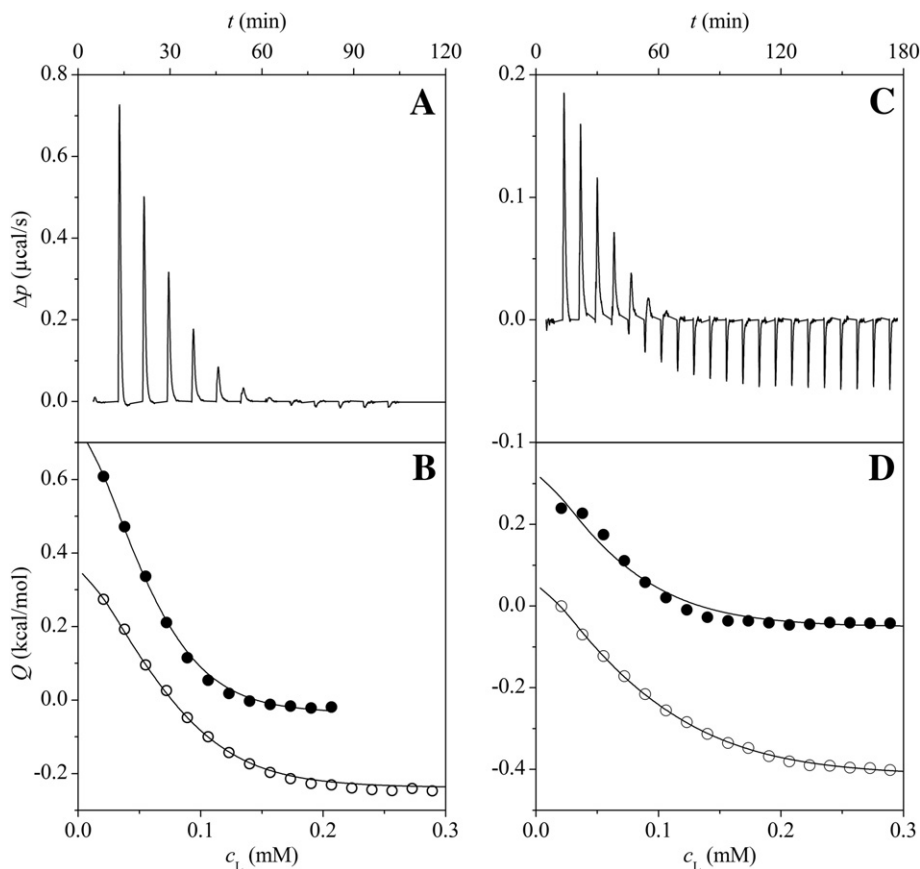

Fig. 5. Exemplary ITC data at 25 °C. LUVs at a total lipid concentration of 10 mM were titrated into the sample cell (1.4448 ml) containing either 25 μM GS (A,B) or 60 μM GS10 (C,D). The initially endothermic heat of reaction decreased and leveled off at a constant heat of dilution as virtually all of the peptides in the sample cell became adsorbed to the lipid vesicles. Top panels (A,C): Baseline-corrected thermograms depicting differential heating power, Δp, versus time, t, obtained upon titration with pure POPC LUVs. Bottom panels (B,D): Normalized and integrated reaction heats, Q, versus lipid concentration in the sample cell, c_L, as derived from titrations with LUVs composed of pure POPC (*solid symbols*) or a 6:4 POPC:Chol mixture (*open symbols*). Also shown are the best fits to the experimental data in terms of a surface partition equilibrium modulated by electrostatic effects ([34]; see Table 1 for fitting parameters).

lines and data points. The K_0 values and derived thermodynamic parameters calculated for the association of GS and GS10 with POPC, POPC/POPG and POPC/Chol LUVs are presented in Table 1.

The first general result evident from Table 1 is that the K_0 values for both peptides in all three LUVs are very high, clustering around $1–2 \times 10^7$/M, indicating that both peptides partition very strongly into all three phospholipid bilayer systems. Examination of the associated thermodynamic parameters reveals that the high negative $\Delta G°$ values for peptide partitioning are due primarily to a very favorable entropy change which is opposed by a much smaller unfavorable change in enthalpy. This indicates that these antimicrobial peptides are driven into phospholipid bilayer membranes primarily by hydrophobic interactions [44]. Also, the K_0 value for the partitioning of GS into these LUVs is about half that of GS10, due to a less favorable change in enthalpy, albeit partially compensated for by a more favorable entropy change. Thus GS10 is more strongly associated with these lipid model membranes, despite its higher solubility in water. Finally, the presence of the negatively charged POPG in mixed POPC/POPG LUVs appears to decrease K_0 values modestly, particularly for GS10, as does the presence of Chol in POPC/Chol vesicles, due primarily to slightly more unfavorable enthalpy change. These same trends were observed in the POPG and POPG/Chol vesicles, although the K_0 values obtained were less reliable (data not presented).

3.6. Size of pure and peptide-bound LUVs

It has been suggested previously that GS may induce phospholipid vesicle fusion or even solubilize phospholipid, at least at higher concentrations of peptide [9–11]. In order to check the integrity of the LUVs exposed to GS10 and to evaluate whether such effects contribute significantly to the ITC data presented above, dynamic light scattering measurements were performed on both control vesicles (LUVs titrated into buffer solution without peptide) and on the sample vesicles (LUVs titrated into the peptide-containing buffer). The data are presented in Table 2. Although the hydrodynamic diameters (d) of the peptide-exposed lipid vesicles are always slightly greater than those of pure lipid vesicles, these results indicate that the various LUVs studied here remain largely intact and do not undergo extensive fusion in the presence of GS10 under the experimental conditions employed in our ITC measurements.

4. Discussion

It is clear that the changes in amino acid composition which transformed GS into GS10 have increased the aqueous solubility of the molecule (see HPLC data) without drastically altering the conformational properties of the peptide, as intended. However, these changes in amino acid composition have affected somewhat other physicochemical properties of GS10, as well as its capacity to interact with both

model and biological membranes. In particular, these modifications have reduced both the content and the solvent inducibility of the secondary structure of GS10 relative to GS. This finding seems inconsistent with the considerable body of experimental evidence indicating that the conformation of the GS ring system is remarkably stable and quite resistant to both thermal and solvent-induced change [9,10,45,46]. However, a plausible explanation for these observations was suggested by ^{1}H NMR and molecular modeling studies of the GS ring-size analogs GS14 and GSdK14 [20,21]. A comparison of the NMR solution structures of GSdK14 obtained in water and TFE/water indicates that the orientation of the antiparallel-aligned VKLKV and LKVKL β-sheet sequences changes with the polarity of the solvent, such that the formation of cross-ring hydrogen bonds becomes more favorable as the TFE content of the solvent increases. Thus, the main difference between the conformations obtained in water and in TFE-containing media arises predominantly from changes in the relative orientations of the β-sheet segments of the peptide and not from changes in secondary structure *per se*. Moreover, our molecular modeling studies indicate that the deviation from the geometry favoring cross-ring H-bonding which occurs when the polarity of solvent increases also promotes closer contacts between the hydrophobic side chains of the molecule, suggesting that this process is driven by thermodynamic tendencies towards minimizing contacts between the hydrophobic surfaces and water. We therefore suggest that the occurrence of comparable phenomena in the GS and GS10 ring systems can also account for the apparent conformational sensitivity of these peptides to changes in solvent polarity, and for the fact that GS is more sensitive than GS10 in this regard, since the greater hydrophobicity of GS will provide a stronger driving force towards reorienting its antiparallel β-sheets when the polarity of the solvent changes.

Our ^{31}P NMR spectroscopic studies clearly indicate that GS10 exhibits a lower propensity for inducing inverted cubic phases in DPEPE membranes than does GS, suggesting that GS10 has a lower propensity than GS for increasing negative monolayer curvature stress in cell membranes (the most probable mechanism underlying membrane disruption by these peptides) [14,15]. This observation is consistent with the results of our *A. laidlawii* B growth inhibitory studies and with previously published studies of the antimicrobial activities of GS and GS10

Table 2
Hydrodynamic diameter of pure and the peptide-bound LUVs.

Model membrane	Hydrodynamic diameter (d), nm	
	In buffer	In GS10 solution
POPC	166	173
POPG	178	185
POPC:POPG (3:1)	179	185
POPC:Chol (6:4)	210	217
POPG:Chol (6:4)	179	190

Table 1
Thermodynamic parameters for the partitioning of GS and GS10 into LUVs of various lipid compositions.

Lipid composition	GS				GS10			
	K_0[a] 1/µM	$\Delta G°$ kcal/mol	$\Delta H°$ kcal/mol	$-T\Delta S°$ kcal/mol	K_0[a] 1/M	$\Delta G°$ kcal/mol	$\Delta H°$ kcal/mol	$-T\Delta S°$ kcal/mol
POPC	12 (11–14)	−12.0	3.4	−15.4	28 (21–37)	−12.5	0.8	−13.4
POPC:POPG (3:1)	8.2 (7.2–9.5)	−11.8	3.7	−15.5	9.3 (7.6–11)	−11.9	1.6	−13.5
POPC:Chol (6:4)	9.1 (7.8–11)	−11.9	3.2	−15.1	18 (17–19)	−12.3	1.4	−13.7

[a] Hydrophobic mole ratio partition coefficient, K_0, standard molar Gibbs free energy, $\Delta G°$, molar transfer enthalpy, $\Delta H°$, and entropic contribution, $-T\Delta S°$, as obtained from ITC experiments performed at 25 °C. Isotherms such as those in Fig. 5 were generated from ITC raw data with the aid of the public-domain software NITPIC [42] and analyzed in terms of a surface partition equilibrium modulated by electrostatic effects [34] by using nonlinear least-squares fitting [43]. The peptide charge number was fixed at +2, and only the outer membrane leaflet was assumed to be accessible to the peptide. Numbers in parentheses indicate 95% confidence intervals obtained by error-surface projection [51].

against various conventional walled bacteria [20,21]. However, given the overall similarities in the structure, conformation and size of the GS and GS10 molecules, it might seem unlikely that GS10 is inherently markedly less disruptive of lipid bilayer integrity than GS itself. Thus, it may be that the apparently lower propensity for GS10 to induce cubic phases in DPEPE bilayers is primarily reflecting its higher aqueous solubility and concomitant lower propensity for partitioning into DPEPE membranes compared to GS, although GS10 binds more strongly to zwitterionic POPC LUVs than does GS. Nevertheless, because of its intrinsically lower hydrophobicity and lower amphipathicity, and the fact that Tyr side chains have a greater affinity for membrane polar/apolar interfaces than Phe side chains [47–50], GS10 could be inherently less disruptive than GS because it may not be able to penetrate as deeply into lipid bilayer membranes as GS. Consequently, we cannot exclude the possibility that there are differences between the inherent membrane-disruptive capacities of GS and GS10 which could be large enough to make a significant contribution to our experimental observations. This aspect of the behavior of these antimicrobial peptides (and many others) is currently unclear and the issue will probably remain unresolved until more precise information on the partitioning and depth of penetration of these peptides into lipid bilayer membranes can be obtained.

Another interesting aspect of our ^{31}P NMR spectroscopic data is the demonstration that membrane Chol attenuates the capacity of both GS and GS10 to induce cubic phase formation in DPEPE membranes. This phenomenon has been observed previously [17], and represents one of the mechanisms whereby effective discrimination between bacterial and animal cell membranes can occur [25,26]. Interestingly, however, the ^{31}P NMR spectroscopic data also indicate that membrane Chol-induced attenuation of the membrane-disruptive tendencies of GS10 appears to be more pronounced than observed with GS itself. Thus, the capacity of membrane Chol to attenuate the membrane-disruptive activities of peptides such as these is also dependent upon the physicochemical properties of the peptide. This conclusion is also supported by the results of our earlier and our present ITC studies, which suggest that this effect may be attributable to a small differential reduction of the binding of these peptides to Chol-rich phospholipid membranes. It should therefore be feasible to exploit this property to design more therapeutically useful GS analogs (see below).

The decreased ability of GS10 to inhibit the growth of the cell wall-less prokaryote A. laidlawii B relative to GS itself is also consistent with previous measurements of the antimicrobial activities of these two peptides [20,21,30]. The results of these growth inhibitory studies are positively correlated with the results of all of the physicochemical studies presented here except for the ITC results, and, because of the absence of a cell wall in A. laidlawii B, these data may even be more accurately reflecting the intrinsic propensities of these peptides to disrupt the lipid bilayers of natural bacterial membranes. As noted above, our RP-HPLC data provide indicate that GS10 is less hydrophobic than GS, that it has a weaker tendency to aggregate in aqueous solution, and that it has lower propensity for interaction with hydrophobic surfaces than does GS. Consequently, GS10 should partition less strongly into the polar/apolar interfacial regions of the lipid bilayers of the cytoplasmic membranes of A. laidlawii B and conventional cell wall-containing bacteria than would GS itself. However, this conclusion is not supported by the results of our ITC studies of the interactions of these peptides with lipid bilayers, since GS10 binds more strongly than GS to all of the phospholipid model membrane systems studied here. Therefore, it appears that differences in the detailed chemical structures of these two antimicrobial peptides, rather than differences in their overall physical properties, may determine their antimicrobial potency and toxicity.

A discussion of our ITC results for the binding of GS10 to various phospholipid vesicles systems (unpublished data) and those obtained previously for GS itself for these same phospholipid bilayers [25], but analyzed without correcting for electrostatic effects, indicates that GS10 binds more strongly and to a greater extent to zwitterionic POPC LUVs than does GS, but that GS10 binds less strongly and to a smaller extent to anionic POPG LUVs than does GS. Moreover, the presence of Chol in either POPC or POPG vesicles produces a much greater decrease in the degree and extent of GS10 binding than is the case for GS. Thus, the binding of GS10 is much less sensitive to the charge of the phospholipid vesicle, but much more sensitive to the order of the phospholipid vesicles as determined by Chol content, than is GS itself. The stronger binding of GS10 to zwitterionic POPC LUVs relative to GS can be attributed primarily to a smaller positive ΔH value for peptide binding, and the weaker binding of GS10 to anionic POPG LUVs relative to GS is due primarily to smaller positive ΔS and $T\Delta S$ values. Similarly, the markedly reduced binding of GS10 to Chol-containing POPC LUVs relative to GS is also due primarily to a larger positive ΔH value, while the decreased binding of GS10 to anionic POPG LUVs relative to GS is due primarily to reduced positive ΔS and $T\Delta S$ values. Overall, the ΔH values for GS10 binding to various phospholipid vesicle systems vary over a greater range than for GS binding to these same systems, while the variations in the range of the ΔS and $T\Delta S$ values with phospholipid and Chol composition are comparable for both peptides. Since the results of studies of antimicrobial potency and hemolytic activity cannot really be corrected for electrostatic effects, the results of our previous ITC studies may be more relevant to the biological activities of these peptides, albeit at the cost of mechanistic and thermodynamic rigor.

It is also interesting to compare the results of our recent ITC studies of the binding of GS14dK$_4$ [26], a diastereomeric lysine ring-size analog of GS, and of GS itself [25], to these obtained in the present ITC study of GS10 binding to phospholipid vesicles of comparable compositions. In general, the strength of binding of GS14dK$_4$ is much more significantly influenced by the phospholipid and Chol composition of the LUVs, in particular by phospholipid surface charge density and Chol-induced ordering of the phospholipid bilayer, than is the binding of GS10 and GS. For example, the binding of GS14dK$_4$ to zwitterionic POPC LUVs is somewhat weaker than that of GS10 but much weaker than that of GS, and GS14dK$_4$ does not exhibit detectable binding to POPC/Chol (3:2) LUVs, whereas GS10 and GS binding to POPC LUVs is only weakened moderately or little, respectively, by the presence of Chol. In contrast, GS14dK$_4$ binds only slightly less tightly to anionic POPG LUVs than does GS, although the binding of GS14dK$_4$ to POPG/Chol (3:2) LUVs is markedly reduced, while the binding of GS10 and GS to POPG LUVs is moderately and little affected by the presence of Chol, respectively. Moreover, the binding of GS14dK$_4$ to all phospholipid vesicles studied is accompanied by much higher positive ΔH values, but also much larger ΔS and $T\Delta S$ values, than is GS10 and especially GS binding, such that the affinity and ΔG values for binding for GS14dK$_4$ vary over a much larger range in different lipid vesicles than is the case for either GS10 or GS.

In principle, many of the ITC data discussed above can be rationalized by a consideration of the relative sizes and charge densities of the GS14dK$_4$, GS10 and GS molecules. Since GS14dK$_4$ is considerably larger than is GS10 or GS, it should be more energetically costly to insert this peptide molecule into phospholipid vesicles, particularly those not bearing a negative surface charge and those exhibiting Chol-induced decreases in fluidity and increases in order, as is indeed observed. This suggestion is supported by the relatively much higher positive ΔH values associated with GS14dK$_4$ binding to phospholipid vesicles, particularly those containing Chol. In contrast, the larger size of the GS14dK$_4$ molecule, and the fact that the somewhat polar and charged D-Lys residue projects toward to hydrocarbon chains of the phospholipid molecules rather than toward the polar headgroups, would tend to more strongly disorder the host phospholipid bilayer, again consistent with the higher ΔS and $T\Delta S$ values observed on the binding of GS14dK$_4$ as compared to GS, particularly in Chol-containing phospholipid vesicles. On the other hand, the GS14dK$_4$ molecule contains three positively charged Lys residues positioned to interact with the phospholipid polar headgroups, while GS10 and GS contain only two positively charged Lys or Orn residues so positioned. Thus GS14dK$_4$ binding to

anionic phospholipid vesicles through increased electrostatic interactions might not be reduced as greatly compared to GS itself, despite its larger size, as in the case of zwitterionic phospholipid vesicles. These results would largely explain the retained antimicrobial activity but greatly reduced hemolytic activity of GS16dK$_4$ as compared to GS and GS10.

Acknowledgements

References

[1] E.J. Prenner, R.N. Lewis, R.N. McElhaney, The interaction of the antimicrobial peptide gramicidin S with lipid bilayer model and biological membranes, Biochim. Biophys. Acta 1462 (1999) 201–221.

[2] T. Ganz, R.I. Lehrer, Antimicrobial peptides in innate immunity, in: K. Lohner (Ed.), Development of Novel Antimicrobial Agents: Emerging Strategies, Horizon Scientific Press, Wymondham, UK, 2001, pp. 139–147.

[3] M. Zasloff, The commercial development of the antimicrobial peptide Pexiganan, in: K. Lohner (Ed.), Development of Novel Antimicrobial Agents: Emerging Strategies, Horizon Scientific Press, Wymondham, UK, 2001, pp. 261–270.

[4] R.M. Hall, C.M. Collis, Origins and evolution of antibiotic and multiple antibiotic resistance in bacteria, in: K. Lohner (Ed.), Development of Novel Antimicrobial Agents: Emerging Strategies, Horizon Scientific Press, Wymondham, UK, 2001, pp. 1–15.

[5] K. Lohner, E. Staudegger, Are we on the threshold of the post-antibiotics era? in: K. Lohner (Ed.), Development of Novel Antimicrobial Agents: Emerging Strategies, Horizon Scientific Press, Wymondham, UK, 2001, pp. 149–165.

[6] R.M. Epand, H.J. Vogel, Diversity of antimicrobial peptides and their mechanisms of action, Biochim. Biophys. Acta 1462 (1999) 11–28.

[7] N. Sitaram, R. Nagaraj, Interaction of antimicrobial peptides with biological and model membranes: structural and charge requirements for activity, Biochim. Biophys. Acta 1462 (1999) 29–54.

[8] G.G. Gause, M.G. Brazhnikova, Gramicidin S and its use in the treatment of infected wounds, Nature 154 (1944) 703.

[9] N. Izumiya, T. Kato, H. Aoyaga, M. Waki, M. Kondo, Synthetic Aspects of Biologically Active Cyclic Peptides: Gramicidin S and Tyrocidines, Halsted Press, New York, 1979.

[10] M. Waki, N. Izumiya, Recent advances in the biotechnology of β-lactams and microbial bioactive peptides, in: H. Kleinhaug, H. van Dohren (Eds.), Biochemistry of Peptide Antibiotics, Walter de Gruyter Company, Berlin, 1990, pp. 205–240.

[11] E.J. Prenner, R.N.A.H. Lewis, L.H. Kondejewski, R.S. Hodges, R.N. McElhaney, Biophysical studies of the interaction of the antimicrobial peptide gramicidin S with lipid bilayers and biological membranes, Phys. Can. 60 (2004) 121–129.

[12] E.J. Prenner, R.N. Lewis, L.H. Kondejewski, R.S. Hodges, R.N. McElhaney, Differential scanning calorimetric study of the effect of the antimicrobial peptide gramicidin S on the thermotropic phase behavior of phosphatidylcholine, phosphatidylethanolamine and phosphatidylglycerol lipid bilayer membranes, Biochim. Biophys. Acta 1417 (1999) 211–223.

[13] R. Krivanek, P. Rybar, E.J. Prenner, R.N. McElhaney, T. Hianik, Interaction of the antimicrobial peptide gramicidin S with dimyristoyl–phosphatidylcholine bilayer membranes: a densitometry and sound velocity study, Biochim. Biophys. Acta 1510 (2001) 452–463.

[14] E.J. Prenner, R.N. Lewis, K.C. Neuman, S.M. Gruner, L.H. Kondejewski, R.S. Hodges, R.N. McElhaney, Nonlamellar phases induced by the interaction of gramicidin S with lipid bilayers. A possible relationship to membrane-disrupting activity, Biochemistry 36 (1997) 7906–7916.

[15] E. Staudegger, E.J. Prenner, M. Kriechbaum, G. Degovics, R.N. Lewis, R.N. McElhaney, K. Lohner, X-ray studies on the interaction of the antimicrobial peptide gramicidin S with microbial lipid extracts: evidence for cubic phase formation, Biochim. Biophys. Acta 1468 (2000) 213–230.

[16] R.N. Lewis, E.J. Prenner, L.H. Kondejewski, C.R. Flach, R. Mendelsohn, R.S. Hodges, R.N. McElhaney, Fourier transform infrared spectroscopic studies of the interaction of the antimicrobial peptide gramicidin S with lipid micelles and with lipid monolayer and bilayer membranes, Biochemistry 38 (1999) 15193–15203.

[17] E.J. Prenner, R.N. Lewis, M. Jelokhani-Niaraki, R.S. Hodges, R.N. McElhaney, Cholesterol attenuates the interaction of the antimicrobial peptide gramicidin S with phospholipid bilayer membranes, Biochim. Biophys. Acta 1510 (2001) 83–92.

[18] J. Salgado, S.L. Grage, L.H. Kondejewski, R.S. Hodges, R.N. McElhaney, A.S. Ulrich, Membrane-bound structure and alignment of the antimicrobial beta-sheet peptide gramicidin S derived from angular and distance constraints by solid state ^{19}F NMR, J. Biomol. NMR 21 (2001) 191–208.

[19] M. Ashrafuzzaman, O.S. Andersen, R.N. McElhaney, The antimicrobial peptide gramicidin S permeabilizes phospholipid bilayer membranes without forming discrete ion channels, Biochim. Biophys. Acta 1778 (2008) 2814–2822.

[20] L.H. Kondejewski, S.W. Farmer, D.S. Wishart, C.M. Kay, R.E. Hancock, R.S. Hodges, Modulation of structure and antibacterial and hemolytic activity by ring size in cyclic gramicidin S analogs, J. Biol. Chem. 271 (1996) 25261–25268.

[21] L.H. Kondejewski, M. Jelokhani-Niaraki, S.W. Farmer, B. Lix, C.M. Kay, B.D. Sykes, R.E. Hancock, R.S. Hodges, Dissociation of antimicrobial and hemolytic activities in cyclic peptide diastereomers by systematic alterations in amphipathicity, J. Biol. Chem. 274 (1999) 13181–13192.

[22] M. Jelokhani-Niaraki, L.H. Kondejewski, S.W. Farmer, R.E. Hancock, C.M. Kay, R.S. Hodges, Diastereoisomeric analogues of gramicidin S: structure, biologicalactivity and interaction with lipid bilayers, Biochem. J. 349 (Pt 3) (2000) 747–755.

[23] L.H. Kondejewski, D.L. Lee, M. Jelokhani-Niaraki, S.W. Farmer, R.E. Hancock, R.S. Hodges, Optimization of microbial specificity in cyclic peptides by modulation of hydrophobicity within a defined structural framework, J. Biol. Chem. 277 (2002) 67–74.

[24] D.L. Lee, R.S. Hodges, Structure–activity relationships of de novo designed cyclic antimicrobial peptides based on gramicidin S, Biopolymers 71 (2003) 28–48.

[25] T. Abraham, R.N. Lewis, R.S. Hodges, R.N. McElhaney, Isothermal titration calorimetry studies of the binding of the antimicrobial peptide gramicidin S to phospholipid bilayer membranes, Biochemistry 44 (2005) 11279–11285.

[26] T. Abraham, R.N. Lewis, R.S. Hodges, R.N. McElhaney, Isothermal titration calorimetry studies of the binding of a rationally designed analogue of the antimicrobial peptide gramicidin s to phospholipid bilayer membranes, Biochemistry 44 (2005) 2103–2112.

[27] L.H. Kondejewski, S.W. Farmer, D.S. Wishart, R.E. Hancock, R.S. Hodges, Gramicidin S is active against both gram-positive and gram-negative bacteria, Int. J. Pept. Protein Res. 47 (1996) 460–466.

[28] D.L. Lee, C.T. Mant, R.S. Hodges, A novel method to measure self-association of small amphipathic molecules: temperature profiling in reversed-phase chromatography, J. Biol. Chem. 278 (2003) 22918–22927.

[29] J.R. Silvius, R.N. McElhaney, Lipid compositional manipulation in Acholeplasma laidlawii B. Effect of exogenous fatty acids on fatty acid composition and cell growth when endogenous fatty acid production is inhibited, Can. J. Biochem. 56 (1978) 462–469.

[30] M. Kiricsi, E.J. Prenner, M. Jelokhani-Niaraki, R.N. Lewis, R.S. Hodges, R.N. McElhaney, The effects of ring-size analogs of the antimicrobial peptide gramicidin S on phospholipid bilayer model membranes and on the growth of Acholeplasma laidlawii B, Eur. J. Biochem. 269 (2002) 5911–5920.

[31] T. Wiseman, S. Williston, J.F. Brandts, L.N. Lin, Rapid measurement of binding constants and heats of binding using a new titration calorimeter, Anal. Biochem. 179 (1989) 131–137.

[32] J. Seelig, Titration calorimetry of lipid–peptide interactions, Biochim. Biophys. Acta 1331 (1997) 103–116.

[33] T. Wieprecht, J. Seelig, Isothermal titration calorimetry for studying interactions between peptides and lipid membranes, in: T.J.M. Sidney, A. Simon (Eds.), Curr. Top. Membr., vol. 52, Academic Press, 2002, pp. 31–56.

[34] S. Keller, H. Heerklotz, A. Blume, Monitoring lipid membrane translocation of sodium dodecyl sulfate by isothermal titration calorimetry, J. Am. Chem. Soc. 128 (2006) 1279–1286.

[35] C.T. Mant, Y. Chen, R.S. Hodges, Temperature profiling of polypeptides in reversed-phase liquid chromatography. I. Monitoring of dimerization and unfolding of amphipathic alpha-helical peptides, J. Chromatogr. A 1009 (2003) 29–43.

[36] C.T. Mant, B. Tripet, R.S. Hodges, Temperature profiling of polypeptides in reversed-phase liquid chromatography. II. Monitoring of folding and stability of two-stranded alpha-helical coiled-coils, J. Chromatogr. A 1009 (2003) 45–59.

[37] Y. Chen, C.T. Mant, S.W. Farmer, R.E. Hancock, M.L. Vasil, R.S. Hodges, Rational design of alpha-helical antimicrobial peptides with enhanced activities and specificity/therapeutic index, J. Biol. Chem. 280 (2005) 12316–12329.

[38] Z. Jiang, B.J. Kullberg, H. van der Lee, A.I. Vasil, J.D. Hale, C.T. Mant, R.E. Hancock, M.L. Vasil, M.G. Netea, R.S. Hodges, Effects of hydrophobicity on the antifungal activity of alpha-helical antimicrobial peptides, Chem. Biol. Drug Des. 72 (2008) 483–495.

[39] W. Hartsock, R.S. Hodges, Rational design of amphipathic α-helical and cyclic β-sheet antimicrobial peptides: specificity and therapeutic potential, in: M. Castanho, N. Santos (Eds.), Peptide Drug Discovery and Development: Translational Research in Academia and Industry, Wiley-VCH, Weinheim, Germany, 2011, pp. 91–117.

[40] R.S. Hodges, Z. Jiang, J. Whitehurst, C.T. Mant, Development of antimicrobial peptides as therapeutic agents, in: S.C. Gad (Ed.), Development of Therapeutic Agents Handbook, John Wiley and Sons Inc., Hoboken, New Jersey, 2011, pp. 285–358.

[41] M. Jelokhani-Niaraki, E.J. Prenner, L.H. Kondejewski, C.M. Kay, R.N. McElhaney, R.S. Hodges, Conformation and other biophysical properties of cyclic antimicrobial peptides in aqueous solutions, J. Pept. Res. 58 (2001) 293–306.

[42] S. Keller, C. Vargas, H. Zhao, G. Piszczek, C.A. Brautigam, P. Schuck, High-precision isothermal titration calorimetry with automated peak-shape analysis, Anal. Chem. 84 (2012) 5066–5073.

[43] C. Vargas, J. Klingler, S. Keller, Membrane partitioning and translocation studied by isothermal titration calorimetry, Methods Mol. Biol. 1033 (2013) 253–271.

[44] C. Tanford, Biophysical Chemistry: Part I: The Conformation of Biological Macromolecules, Chapter 5, in: C.R. Cantor, P.R. Schimmel (Eds.), W. H. Freeman, San Francisco, CA, 1980.

[45] C. Yu, J.F. Hwang, C.J. Yeh, L.C. Chuang, Solution conformation of gramicidin S determined by nuclear magnetic resonance and distance geometry calculation, J. Chin. Chem. Soc. 39 (1992) 231–234.

[46] D. Mihailescu, J.C. Smith, Molecular dynamics simulation of the cyclic decapeptide antibiotic, gramicidin S, in dimethyl sulfoxide solution, J. Phys. Chem. B 103 (1999) 1586–1594.

[47] W.M. Yau, W.C. Wimley, K. Gawrisch, S.H. White, The preference of tryptophan for membrane interfaces, Biochemistry 37 (1998) 14713–14718.

[48] A. Senes, D.C. Chadi, P.B. Law, R.F. Walters, V. Nanda, W.F. Degrado, E(z), a depth-dependent potential for assessing the energies of insertion of amino acid side-chains into membranes: derivation and applications to determining the orientation of transmembrane and interfacial helices, J. Mol. Biol. 366 (2007) 436–448.

[49] W.C. Wimley, S.H. White, Experimentally determined hydrophobicity scale for proteins at membrane interfaces, Nat. Struct. Biol. 3 (1996) 842–848.

[50] W.C. Wimley, T.P. Creamer, S.H. White, Solvation energies of amino acid side chains and backbone in a family of host–guest pentapeptides, Biochemistry 35 (1996) 5109–5124.

[51] G. Kemmer, S. Keller, Nonlinear least-squares data fitting in Excel spreadsheets, Nat. Protoc. 5 (2010) 267–281.